Published in final edited form as:
Cell Rep. 2014 September 11; 8(5): 1533–1544. doi:10.1016/j.celrep.2014.07.048.

Contractile ring stability in *S. pombe* depends on F-BAR protein Cdc15p and Bgs1p transport from the Golgi complex

Rajesh Arasada[1] and **Thomas D. Pollard**[1,2,3,*]

[1]Department of Molecular Cellular and Developmental Biology, Yale University, PO Box 208103, New Haven, CT 06520-8103 USA,

[2]Department of Molecular Biophysics and Biochemistry, Yale University, PO Box 208103, New Haven, CT 06520-8103 USA,

[3]Department of Cell Biology, Yale University, PO Box 208103, New Haven, CT 06520-8103 USA,

Summary

Cdc15p is known to contribute to cytokinesis in fission yeast; however, the protein is not required to assemble the contractile ring of actin and myosin, but helps to anchor the ring to the plasma membrane. Cdc15p has a lipid binding F-BAR domain, suggesting that it provides a physical link between the plasma membrane and contractile ring proteins. However, we find that a more important function of Cdc15p during cytokinesis is to help deliver a transmembrane enzyme, Bgs1p (also called Cps1p), from the Golgi apparatus to the plasma membrane, where it appears to anchor the contractile ring. Bgs1p synthesizes the cell wall in the cleavage furrow, but its enzyme activity is not required to anchor the contractile ring. We estimate that ~2000 Bgs1p molecules are required to anchor the ring. Without Bgs1p anchors, contractile rings slide along the plasma membrane, a phenomenon that depends on an unconventional type II myosin called Myp2p.

Introduction

Cytokinesis by fission yeast *S. pombe* depends on the formation and constriction of a contractile ring and septum formation. Preparation for cytokinesis begins during interphase with the formation of cortical protein assemblies called nodes (Martin and Berthelot-Grosjean, 2009; Moseley et al., 2009). Proteins required for the assembly, maturation and constriction of the contractile ring are recruited to nodes in an orderly fashion beginning during interphase (Pollard and Wu, 2010; Wu et al., 2003). A signaling pathway called the Septation Initiation Network (SIN) controls the assembly of the septum (Balasubramanian et al., 1998; Le Goff et al., 1999a). During the time the contractile ring matures, SIN initiates recruitment of β-glucan synthetases Bgs1p (*cps1*$^+$), Bgs4p (*bgs4*$^+$) and Ags1p (*mok1*$^+$) to the plasma membrane next to the contractile ring, where these integral membrane proteins

*Corresponding author: thomas.pollard@yale.edu; telephone 203-432-3565; fax 203-432-6060.

synthesize the septum (Cortes et al., 2005; Cortes et al., 2002; Cortes et al., 2012). In cells with mutations in SIN signaling or *cps1*$^{+}$ many contractile rings are not centered, suggestive of an anchoring defect, and others are unstable and disappear without constricting (Hachet and Simanis, 2008; Le Goff et al., 1999b; Liu et al., 2002; Liu et al., 1999; Roberts-Galbraith et al., 2010). The Post Anaphase Array of microtubules (PAA) assembles during the maturation period near the contractile ring and contributes to anchoring the contractile ring (Pardo and Nurse, 2003), but the molecules anchoring the contractile ring to the membrane are not known.

We turned to the essential F-BAR protein Cdc15p as a potential anchor. This phosphoprotein is required for efficient endocytosis when phosphorylated (Arasada and Pollard, 2011) and for cytokinesis when dephosphorylated (Carnahan and Gould, 2003; Fankhauser et al., 1995). Temperature sensitive mutations of *cdc15*$^{+}$ compromise cytokinesis, but clarity about the nature of the defects has emerged slowly. The presence of incomplete contractile rings in fixed mutant cells (Arai and Mabuchi, 2002; Balasubramanian et al., 1998; Carnahan and Gould, 2003; Fankhauser et al., 1995) and the ability of Cdc15p to interact with a cytokinesis formin Cdc12p (Carnahan and Gould, 2003; Roberts-Galbraith et al., 2010) suggested a role in the contractile ring assembly. Other evidence suggests that Cdc15p acts later during cytokinesis. For example, Δ*cdc15* cells lacking Cdc15p can assemble contractile rings that fail to constrict and separate the daughter cells (Wachtler et al., 2006), Cdc15p continues to accumulate in contractile rings during the maturation period (Wu and Pollard, 2005), some proteins that interact with Cdc15p (ethanol dependent protein Etd1p (Daga et al., 2005), paxillin Pxl1p (Ge and Balasubramanian, 2008; Pinar et al., 2008) and transglutaminase-like protein Cyk3p (Pollard et al., 2012)) accumulate in the cleavage furrow after the ring forms and cells lacking the C-terminal SH3 domain of Cdc15p assemble contractile ring but fail to anchor them (Roberts-Galbraith et al., 2009).

Here we find that Cdc15p associates with *trans*-Golgi membranes through its middle domain (residues 298–868). When Cdc15p is mutated or depleted from cells or the Clp1p phosphatase is deleted, the septation enzyme Bgs1p is transported slowly from the *trans*-Golgi network to the plasma membrane. During this delay, normally formed contractile rings slide from the center of the cell in a manner dependent on Myp2p (unconventional myosin-II), so cleavage furrows are misplaced. The enzyme activity of Bgs1p is not required to anchor the contractile ring.

Results

Mutations in the F-BAR protein Cdc15p and the phosphatase Clp1p result in contractile ring sliding during cytokinesis

We used three approaches to investigate the role of the essential F-BAR protein Cdc15p during cytokinesis. (i) We repressed expression of Cdc15p in *41xnmt1cdc15* cells for 24 h with 2.8 μM thiamine reducing the whole cell concentration from 12 μM to 0.2 μM (Arasada and Pollard, 2011), so hereafter we call these cells “depleted of Cdc15p”. (ii) We used a strain with the single SH3 domain deleted from Cdc15p (Roberts-Galbraith et al., 2009), hereafter called *cdc15*Δ*SH3* cells. (iii) We deleted the gene for the Clp1p phosphatase

(Trautmann et al., 2001) that regulates Cdc15p as well as many other phosphorylated proteins (Chen et al., 2013). We followed contractile ring assembly in time lapse movies of cells expressing the myosin-II regulatory light chain, Rlc1p, tagged in the genome on the C-terminus with red fluorescent protein tdTomato. We report results using the cell cycle time scale (Wu et al., 2003) where zero is the time of spindle pole body separation or appearance of spindle microtubules.

The three mutant strains had slightly different cytokinesis defects. Septa were located within 5% of the middle of all wild type cells, but were displaced further from the middle in 20–60% of cells depleted of Cdc15p, *cdc15ΔSH3* cells and Δ*clp1* cells (Figure 1A, B). Furthermore 30% of cells depleted of Cdc15p had multiple septa and a few were branched (Figure 1A), defects not observed in *cdc15ΔSH3* or Δ*clp1* cells.

Contractile rings assembled normally in the middle of cells depleted of Cdc15p and Δ*clp1* mutants, but many divided asymmetrically, because the rings slid away from the center toward a pole (Figure 1C) as originally observed for *cdc15ΔSH3* cells (Roberts-Galbraith et al., 2009). Wild type cells, cells depleted of Cdc15p, *cdc15ΔSH3* mutant cells and Δ*clp1* mutant cells all concentrated Rlc1p-tdTomato in precursor nodes around the cell equator between −12 to −4 min and condensed these nodes into contractile rings between times +4 to +16 min (Figure 1C – 1F). Fully formed contractile rings in wild type cells were stationary as they matured for 20 min before beginning to constrict between times +22 to +35 min. On the other hand, starting at time +16 min contractile rings moved steadily away from the cell center at about 0.1 μm/min in ~80% of cells depleted of Cdc15p (Movie 1), 45% of *cdc15ΔSH3* cells and 45% of Δ*clp1* cells (Figures 1C – 1F). Even in movies taken at 1 s intervals rings appeared to slide away from the cell center in cells depleted of Cdc15p (Movie 2) rather than changing position by cycles of assembly and disassembly at different positions.

Sliding rings in cells depleted of Cdc15p had two fates. About half stalled and began to constrict after time +46 min resulting in a septum between daughter cells of different sizes (Figure 1D). Cytokinesis failed in other cells, because their rings disassembled as they moved toward a cell tip (Figure 1D). The cytokinesis phenotype was less severe in *cdc15ΔSH3* and Δ*clp*1 cells, because contractile rings did not slide to the cell tip but stalled and constricted, forming daughter cells of different sizes (Figures 1B and 1C). None of these *cdc15ΔSH3* cells and Δ*clp1* cells formed multiple septa or failed to complete abscission. Initial rates of ring constriction were faster in wild type cells (0.83 μm/min) than cells depleted of Cdc15p (0.3 μm/min), *cdc15ΔSH3* cells (0.47 μm/min) or Δ*clp1* cells (0.62 μm/min) (Figure 1G).

Cells depleted of Cdc15p recruit Cdc12p to the equator and assemble normal post anaphase microtubule arrays

Although Cdc15p interacts directly with formin Cdc12p and the two proteins are reported to depend on each other to localize in contractile rings (Carnahan and Gould, 2003; Roberts-Galbraith et al., 2010), Cdc12p-3YFP accumulated normally in nodes and contractile rings of cells depleted of Cdc15p. In both wild type cells and cells depleted of Cdc15p, Cdc12p-3YFP concentrated in small nodes around the cell center by time +1 min, and by

time +15 min these nodes condensed into complete contractile rings with ~350 molecules of Cdc12p (Figure 2A and 2B). Cytoplasmic concentrations of Cdc12p were 0.043 μM in wild type cells and 0.041 μM in cells depleted of Cdc15p.

Rings that constricted in wild type cells and in cells depleted of Cdc15p retained the full complement of ~300 Cdc12p molecules until the formin dissociated in parallel with constriction (compare Figures 2A and 2B). Cdc12p dissociated prematurely from contractile rings that failed to constrict in cells depleted of Cdc15p (Figure 2B and 2C).

We looked for an effect of the *cdc15* mutations on the post anaphase array of microtubules, because they help retain the contractile ring at the cell center (Pardo and Nurse, 2003) and Myp2p is linked to their placement near the contractile ring (Samejima et al., 2010). In cells depleted of Cdc15p the post anaphase array of microtubules assembled at the normal time near the equator as the primary septum formed (Figure S1).

Defects in contractile ring anchoring in *cdc15*$^{+}$ mutant cells are caused by slow delivery of Bgs1p to the cleavage site

Previous work showed that septum deposition participates in constriction and anchoring of the contractile ring (Clifford et al., 2008; Cortes et al., 2002; Hachet and Simanis, 2008; Le Goff et al., 1999b; Liu et al., 2002; Liu et al., 1999; Roberts-Galbraith et al., 2010). Our microscopic and biochemical experiments link the cytokinesis defects in *cdc15* and Δ*clp1* mutant cells to the transmembrane glucan synthetase Bgs1p.

Figure 3 traces the localization of Bgs1p around the cell cycle in wild type cells. The enzyme normally moves from the secretory pathway to the cleavage furrow for cytokinesis (Figure 3A). During interphase GFP-Bgs1p concentrated at both poles, but was also present in randomly distributed cytoplasmic puncta between the poles. The presence of Sec72p and clathrin light chain Clc1p identified these puncta as clathrin coated *trans*-Golgi compartments (Figure S3) (Vjestica et al., 2008). During mitosis GFP-Bgs1p relocalized from the poles to the cell center, moving from Sec72p-positive compartments to an equatorial band near the contractile ring. Immediately after cell division most GFP-Bgs1p relocalized to the old growing ends and reappeared in Sec72p-positive puncta (Figures 3A).

All Bgs1p temperature sensitive *cps1–191* mutant cells assembled contractile rings from nodes similar to wild type cells even at restrictive temperatures, but this strain had two cytokinesis defects (Figures 3B – 3D). First, 40% of contractile rings slid towards a cell tip. Second, the onset of ring constriction was delayed. At 25°C constriction began in wild type cells at +27 ± 1.6 min, but was delayed to +56.5 ± 16.5 min in *cps1–191* cells (Figure 3B). At the restrictive temperature contractile ring was delayed from time +17.5 ± 1.5 min to +73.5 ± 24.5 min in *cps1–191* cells and only 40% of stationary and sliding rings (Figure 3C).

Since both *cdc15*$^{+}$ and *cps1*$^{+}$ mutations resulted in sliding contractile rings, we investigated how Bgs1p and its product, the septum, are related to this phenotype. Careful measurements revealed that appearance of GFP-Bgs1p at the cleavage site is slow in cells depleted of Cdc15p, *cdc15*Δ*SH3* mutants and Δ*clp1* mutants and that rings slide until GFP-Bgs1p

reaches a critical level (Figure 4). We used two methods to measure the transfer of GFP-Bgs1p from the Golgi apparatus to the plasma membrane adjacent to the contractile ring.

In Figure 4B we used fluorescence intensity to count the number GFP-Bgs1p molecules around the equator (open symbols). Cytoplasmic puncta containing both GFP-Bgs1p and Sec72p first appeared near the contractile ring at time +15 ± 2 min in wild type cells, and GFP-Bgs1p accumulated in a band around the equator at ~500 molecules per min, reaching ~2,000 molecules by time +22 min and ~4500 molecules by time +27 min, when contractile rings began to constrict (Figure 4A and 4B). In the mutant cells vesicles containing GFP-Bgs1p accumulated normally near the contractile ring at time +14.4 ± 2.6 min in cells depleted of Cdc15p, 16.3 ± 2.4 min in *cdc15*Δ*SH3* cells and 17.8 ± 5.3 min in Δ*clp1* cells (Figure 4A and 4B), but the rate of transfer of GFP-Bgs1p to the equatorial band was slower than normal, ~200 molecules per min in cell depleted of Cdc15p, ~400 molecules per min in *cdc15*Δ*SH3* cells and ~150 molecules per min in Δ*clp1*cells.

In Figure 4B–E we identified the time when a clear band of GFP-Bgs1p was established around the equator. The band appeared in wild type cells by time +18.8 ± 1.6 min, 3.7 ± 1.8 min after the accumulation of vesicles (~800 molecules) (Figure 4B and 4C), but was delayed by 12.14 ± 2.4 min in cells depleted of Cdc15p (appearing at +24.5 ± 3.5 min when 700 molecules accumulated) (Figure 4B and 4C), 10.8 ± 2 min in *cdc15*Δ*SH3* cells (appearing at +25.3 min ± 3.3 with ~900 molecules) (Figure 4B and 4D) and by 14.9 ± 2.5 min in Δ*clp1* cells (appearing at 31.8 ± 5 min with 1600 molecules) (Figure 4B and 4E).

Contractile rings slid in all three *cdc15*$^{+}$ mutant strains during the interval between the appearance of Myp2p at about time +20 min (Figure 4B) and the accumulation of 2000 molecules of GFP-Bgs1p (Figure 4B). Rings did not slide in wild type cells where Myp2p and 2000 molecules of Bgs1p both appeared at the same time.

About 4500 molecules of GFP-Bgs1p accumulated at the equator of wild type cells when contractile rings began to constrict at +27 ± 1.6 min. The numbers of equatorial GFP-Bgs1p molecules at the onset of constriction varied in the mutant cells: ~3600 molecules at 32.6 ± 3.2 min in *cdc15*Δ*SH3* cells, ~4500 molecules at 46.5 ± 5.7 min in Δ*clp1* cells and 3,000 molecules at 34.5 ± 4 min in *41xnmt1cdc15* cells (Figure 4B, 4C, 4D and 4E).

After the physical separation of the daughter cells at the end of cell division GFP-Bgs1p relocalized normally to cell tips during interphase in *cdc15*$^{+}$ *and clp1*$^{+}$ mutant cells. Although GFP-Bgs1p appeared to accumulate faster at the old end in cells depleted of Cdc15p, this difference is likely due to the delay or defects in cell separation in these mutant cells (Figure S2).

Inhibition of the catalytic activity of GFP-Bgs1p with Aculeacin A (Yamaguchi et al., 1985) slowed the formation of the contractile ring slightly (Figure 4F) and stopped septum formation (Figure 4I), but GFP-Bgs1p appeared early and accumulated faster than normal in the cleavage furrow, reaching ~2,000 molecules before +20 min (Figure 4B and 4F). The contractile ring remained anchored at the cell center for more than an hour (Figure 4I) and failed to constrict even as ~15,000 molecules of Bgs1p accumulated around the equator (Figure 4B) before dispersing (Figure 4I).

Distinct Cdc15p domains mediate targeting to the cleavage site and association with the Golgi apparatus

We tagged the N-termini of full length and truncation mutants of Cdc15p with mEGFP or mCherry to study how Cdc15p localizes to the Golgi apparatus and cleavage furrow by biochemical fractionation and fluorescence microscopy. We expressed mEGFP-Cdc15p, mCherry-Cdc15p and mCherry-Cdc15pΔSH3 from the endogenous *cdc15*$^{+}$ locus. Constructs mCherry-Cdc15p-FBD$_{1–297}$ (F-BAR domain), mCherry-Cdc15p-MD$_{298–868}$ (middle region between the F-BAR domain and the SH3 domain) and mCherry-Cdc15p-MDSH3$_{298–927}$ (Cdc15p lacking the F-BAR domain) were expressed under the control of the *cdc15*$^{+}$ promoter in the *leu1*$^{+}$ locus of *41xnmt1cdc15* mutant cells depleted of Cdc15p.

During subcellular fractionation only tiny amounts Cdc15p were soluble and the rest divided between low-speed and high-speed pellets. During sedimentation velocity ultracentrifugation of homogenates on 18–60% sucrose gradients (Antebi and Fink, 1992), most mEGFP-Cdc15p sedimented rapidly. This pattern was similar to the sedimentation of clathrin light chain Clc1p-mCherry and the *trans*-Golgi membrane marker Sec72p, the homolog of budding yeast *SEC7 Arf GEF*. GFP-Bgs1p sedimented in two broad peaks with 40% sedimenting slowly and 60% cosedimenting with Cdc15p and Sec72p. The *cis*-Golgi membrane protein Anp1p-mCherry separated into three fractions: ~30% in a slowly sedimenting peak just ahead of the soluble proteins, ~32% sedimented in the middle of the gradient and ~38% sedimenting rapidly with Clc1p-mCherry, Cdc15p and Sec72p (Figure 5A and S4).

Sedimentation velocity experiments showed that mCherry-Cdc15p-MD$_{298–868}$ and all mCherry-Cdc15p constructs that included the middle domain (residues 298–868) cosedimented in a single peak with the fast sedimenting fractions of Sec72p and full length Cdc15p (Figure 5B). Most of the construct consisting of only the F-BAR domain (mCherry-Cdc15p-FBD$_{1–297}$) was in the soluble fractions at the top of the tube and only 15% sedimented with Sec72p (Figure 5B and S4).

Fluorescence micrographs of cells expressing the tagged Cdc15p constructs with domain deletions showed how the three domains of Cdc15p contribute to its localization in cells. The cytoplasmic fluorescence from each construct lacking a domain was higher than full length Cdc15p (Figure 5C – 5E), likely because each deletion compromised binding to intracellular structures.

The F-BAR domain is necessary and sufficient for targeting to the cleavage site. During cell division mCherry-Cdc15p-FBD$_{1–297}$ localized to the equators of *41xnmt1cdc15* cells depleted of Cdc15p (Figure 5C). However, mCherry-Cdc15p-FBD$_{1–297}$ did not compensate for depletion of Cdc15p; contractile rings marked with Rlc1p-tdTomato formed normally by +4 min but slid away from the center of the cell (Figures 5F and 5H). The contrast with the cytoplasmic fluorescence was so poor that we could not be sure if mCherry-Cdc15p-FBD$_{1–297}$ concentrated in actin patches.

The middle domain of Cdc15p is necessary and sufficient for association with the Golgi apparatus. When expressed in cells depleted of Cdc15p, the middle domain construct

mCherry-Cdc15p-$MD_{298–868}$ localized to the nucleus in interphase and to a broad region in the middle of cells starting at time +20 min (Figure 5D, 5G and S3A). The equatorial zone of mCherry-Cdc15p-$MD_{298–868}$ coincided with the vesicles containing GFP-Bgs1p, although the contrast with the high cytoplasmic fluorescence was low (Figures 5G, 5H and S5A). In cells depleted of Cdc15p both GFP-Bgs1p and mCherry-Cdc15p-$MD_{298–868}$ trailed behind sliding contractile rings (Figure 5I).

Cdc15pΔSH3-mCherry lacking the C-terminal SH3 domain localized to the contractile ring (Figure 5E) as shown previously (Roberts-Galbraith et al., 2009). During metaphase Cdc15pΔSH3-mCherry concentrated in the contractile ring well before mEGFP-Bgs1p accumulated at the cell center during anaphase B and in the cleavage furrow at the end of anaphase B (Figure S5B).

Myp2p contributes to ring sliding and constriction in *cdc15*$^+$ mutants—Two observations suggested that unconventional myosin-II, Myp2p, contributes to contractile ring sliding in *cdc15*$^+$ and *clp1*$^+$ mutants. First, the temperature sensitive allele *cdc15–140* was synthetically lethal with Δ*myp2* (Figure 6A). Second, in cells depleted of Cdc15p, *cdc15*Δ*SH3* cells and Δ*clp1*cells contractile rings began to slide during the maturation time (Figure 1D – 1F) about when Myp2p-YFP appeared in rings at time +18 min (Figures 6B and 6C) (Bezanilla et al., 2000; Wu et al., 2003). This is well after the appearance of conventional myosin-II Myo2p (Figure 1D – 1F).

Before the onset of constriction, contractile rings accumulated ~1800 molecules of Myp2p-YFP in wild type cells and 1500 molecules of Myp2p-YFP in *cdc15*Δ*SH3* cells (Figure 6C). Compared with wild type cells, cells depleted of Cdc15p contained 1.7 times more total Myp2p-YFP and their contractile rings accumulated ~ 3-fold more Myp2p (~5300 molecules) (Figure 6C). In these mutant cells Myp2p-YFP was unevenly distributed around contractile rings, and elongated structures containing Myp2p-YFP frequently peeled off from contractile rings (Figure 6D; Movie 3). Similar defects were observed in cells depleted of Cdc15p and expressing Rlc1p-tdTomato, which associates with both Myo2p and Myp2p (Figure 6D and Movie 4).

In cells depleted of Cdc15p contractile rings slid very slowly without Myp2p (35 nm/min vs. ~135 nm/min with Myp2) and none constricted (Figure 6E and 6F). We accumulated cytokinetic cells for these experiments by arresting cells in early S phase with 20 mM hydroxyurea in minimal media for 6 h. After washing out hydroxyurea, the cell cycle resumed for 2 h before imaging. The phenotype was similar in unsynchronized cells.

Myp2p coordinates contractile ring constriction with septum deposition—Although Δ*myp2* cells assembled and began to constrict contractile rings marked with Rlc1p-tdTomato at the same time as wild type cells (Figure 7A and 7B), many of these contractile rings had defects (Martin-Garcia and Valdivieso, 2006). First, owing to irregularities or tilting relative to the long axis of the Δ*myp2* cells, the initial circumferences of many rings were larger than circumferences of the cell (Figure 7C). Second, rings in Δ*myp2* cells constricted slower than normal (Figure 7B), and many became irregular during constriction and septum deposition after time +24 min (Figure 7A and 7C, Movie 5). Third,

during constriction all contractile rings in Δ*myp2* cells were displaced to various degrees laterally from the middle of the cell and many were tilted relative to the long axis of the cell (Figure 7D). Contractile rings in 76% of Δ*myp2* cells constricted to a point, but in the remaining 24% of Δ*myp2* cells contractile rings disassembled and released strands of actomyosin without completing constriction.

Septal growth and ring constriction were uncoordinated in many Δ*myp2* cells (Figure 7D). In 43% of Δ*myp2* cells the ring marked Rlc1p-tdTomato remained very close to the equatorial plane and constricted completely in conjunction with septum formation marked with GFP-Bgs1p (Figure 7D, upper panel). In the remaining 57% of Δ*myp2* cells the contractile ring and associated Bgs1p were displaced to one side of the furrow where the septum grew and closed ahead of the contractile ring. In 33% of Δ*myp2* cells these displaced rings constricted completely before cell separation (Figure 7D, middle panel). In 24% of Δ*myp2* cells constriction of the ring and growth of the septum were initially coordinated, but the ring then moved to one side of the septum (Figure 7D lower panel). Subsequently (48 min in Figure 7D lower panel) the septum appeared to close and separate the daughter cells, while the ring regressed.

Discussion

Previous work established that the F-BAR protein Cdc15p has a role in anchoring the contractile ring to the plasma membrane (Roberts-Galbraith et al., 2010), so if the Cdc15p SH3 domain is deleted, contractile rings slide along the cortex of the cell during telophase. One possible mechanism is that Cdc15p is a physical link between the plasma membrane and the contractile ring, given that it interacts with contractile ring proteins (Carnahan and Gould, 2003; Laporte et al., 2011; Lee and Wu, 2012; Roberts-Galbraith et al., 2009) as well as membrane lipids (Takeda et al., 2004). While this may be true, our observations on cells with mutated or depleted Cdc15p revealed that the underlying defect responsible for contractile ring sliding is slow transfer of β-glucan synthetase Bgs1p (and perhaps other proteins) from the Golgi apparatus to the plasma membrane. Rings slide until ~2000 Bgs1p molecules reach the cell surface where they directly or indirectly anchor the contractile ring. Our findings are consistent with genetic evidence that Bgs1p is required to form a cleavage furrow (Liu et al., 1999). Thus, Cdc15p plays a more important role in the assembly of the septum during late anaphase than in the assembly of the contractile ring.

Bgs1p has attractive features for an anchor including 14 transmembrane helices and two large cytoplasmic domains. Bgs1p also synthesizes the septum, which is also thought to be part of the system that anchors the contractile ring (Pardo and Nurse, 2003). However, Bgs1p can anchor the ring even when an inhibitor of its enzyme activity prevents septum formation. Thus, Bgs1p itself is required to anchor the ring.

We propose that Cdc15p contributes to budding clathrin-coated Sec72p vesicles from the Golgi apparatus (Figure S3). This is a unifying hypothesis, given the well-established role of F-BAR proteins such as Cdc15p in clathrin-mediated endocytosis (Arasada and Pollard, 2011; Berro et al., 2010; Qualmann and Kelly, 2000; Tsujita et al., 2006). This hypothesis is consistent with previous evidence that Bgs1p is transported through the secretory pathway,

such as Brefeldin A inhibiting the concentration of GFP-Bgs1p in the cleavage furrow (Liu et al., 2002) and genetic interactions between mutations in cytokinesis genes and genes required for membrane traffic through the Golgi apparatus (Park et al., 2009; Sammons et al., 2011; Walch-Solimena and Novick, 1999). Similarly, mutations in conserved genes required for vesicular transport in the Golgi apparatus (De Matteis and Luini, 2008; Jaulin et al., 2007; Valente et al., 2012) cause septation defects in fission yeast (Brazer et al., 2000; Mishra et al., 2005).

Cells lacking the Clp1p phosphatase have the same phenotype as depleting Cdc15p or deleting its SH3 domain, support for the importance of Clp1p regulating Cdc15p during cytokinesis. The observation that a hypophosphorylated Cdc15p mutant accumulates in vesicle-like structures at the cell center in interphase (Roberts-Galbraith et al., 2010) suggests that dephosphorylation of Cdc15p may be required for its role in transport out of the Golgi apparatus. Given that Clp1p also acts on proteins involved in vesicular trafficking, transcription and ribosome biogenesis (Chen et al., 2013), complementation experiments with Cdc15p having mutations in its phosphorylation sites will be of interest to understand the Δ*clp1* phenotype and the regulation of Cdc15p during cytokinesis.

Our experiments show that contractile ring anchors resist both lateral forces that produce sliding and centripetal forces that pull the ring away from the plasma membrane. Myp2p appears to put a lateral force on contractile rings, allowing them to slide until the anchors mature. Rings rarely slide in wild type cells, because Bgs1p is recruited shortly after Myp2p, so the conditions for sliding, the presence of Myp2p and low numbers of Bgs1p, exist only transiently. Myp2p also has a role in coordinating ring constriction with septum deposition, since rings in many Δ*myp2* cells pull away from the leading edge of the cleavage furrow. Actin polymerization and other motors such as Myo2p may also contribute to slow sliding in Δ*myp2* cells.

Myp2p may also be connected to the role of microtubules in positioning the contractile ring, since deletion of *myp2+* resulted in the loss of protein Mto1p (*m*icro*t*ubule *o*rganizing protein 1) from the contractile ring (Samejima et al., 2010). Mto1p regulates the γ-tubulin complex (Sawin et al., 2004; Venkatram et al., 2004) and post anaphase array microtubules (Pardo and Nurse, 2003; Venkatram et al., 2004) that contribute in some way to coupling septum deposition to contractile ring constriction (Samejima et al., 2010).

Although Cdc15p is not required for contractile ring assembly according to our own observations and previous work (Arai and Mabuchi, 2002; Balasubramanian et al., 1998; Carnahan and Gould, 2003; Hachet and Simanis, 2008), it likely contributes to late steps in cytokinesis in addition to delivering Bgs1p to the cleavage furrow. For example, the SH3 domain of Cdc15p interacts with and recruits Cyk3p, Fic1p, Etd1p and Pxl1p to completed contractile rings (Daga et al., 2005; Ge and Balasubramanian, 2008; Pinar et al., 2008; Pollard et al., 2012; Roberts-Galbraith et al., 2009). Furthermore, the progressive dephosphorylation of Cdc15p during mitosis (Fankhauser et al., 1995; Roberts-Galbraith et al., 2010; Wachtler et al., 2006) should promote the well-established interaction of Cdc15p with Cdc12p (Carnahan and Gould, 2003; Laporte et al., 2011; Roberts-Galbraith et al., 2010) after contractile rings form.

Experimental Procedures

Supplementary Table 1 lists the strains used in this study. Yeast cells were grown for microscopy in exponential phase at 25°C. Proteins were tagged with fluorescent proteins in the genome and expressed from native promoters in the native loci or inserted in the *leu*$^+$ locus and expressed from native promoters.

Microscopy

Cells were imaged on a thin pad of 25% gelatin in EMM5S medium supplemented with 0.1 mM *n*-propyl-gallate (Arasada and Pollard, 2011) with an Olympus IX-71 microscope with a 100×/NA 1.4 Plan Apo lens (Olympus) and a CSU-X1 (Andor Technology) confocal spinning disk confocal system equipped with an iXON-EMCCD camera (Andor Technology) calibrated to count fluorescent proteins (Wu and Pollard, 2005).

Subcellular Fractionation

Cell lysates were fractionated by sedimentation velocity ultracentrifugation in a sucrose gradient as described for budding yeast (Antebi and Fink, 1992; Barrowman et al., 2010). Proteins were quantitated by immunoblotting with antibodies fluorescent protein tags (Arasada and Pollard, 2011).

Supplementary Material

Refer to Web version on PubMed Central for supplementary material.

References

Antebi A, Fink GR. The yeast Ca(2+)-ATPase homologue, PMR1, is required for normal Golgi function and localizes in a novel Golgi-like distribution. Molecular biology of the cell. 1992; 3:633–654. [PubMed: 1379856]

Arai R, Mabuchi I. F-actin ring formation and the role of F-actin cables in the fission yeast Schizosaccharomyces pombe. Journal of cell science. 2002; 115:887–898. [PubMed: 11870208]

Arasada R, Pollard TD. Distinct roles for F-BAR proteins Cdc15p and Bzz1p in actin polymerization at sites of endocytosis in fission yeast. Current biology : CB. 2011; 21:1450–1459. [PubMed: 21885283]

Balasubramanian MK, McCollum D, Chang L, Wong KC, Naqvi NI, He X, Sazer S, Gould KL. Isolation and characterization of new fission yeast cytokinesis mutants. Genetics. 1998; 149:1265–1275. [PubMed: 9649519]

Barrowman J, Bhandari D, Reinisch K, Ferro-Novick S. TRAPP complexes in membrane traffic: convergence through a common Rab. Nature reviews Molecular cell biology. 2010; 11:759–763.

Berro J, Sirotkin V, Pollard TD. Mathematical modeling of endocytic actin patch kinetics in fission yeast: disassembly requires release of actin filament fragments. Molecular biology of the cell. 2010; 21:2905–2915. [PubMed: 20587776]

Bezanilla M, Wilson JM, Pollard TD. Fission yeast myosin-II isoforms assemble into contractile rings at distinct times during mitosis. Current biology : CB. 2000; 10:397–400. [PubMed: 10753748]

Brazer SC, Williams HP, Chappell TG, Cande WZ. A fission yeast kinesin affects Golgi membrane recycling. Yeast. 2000; 16:149–166. [PubMed: 10641037]

Carnahan RH, Gould KL. The PCH family protein, Cdc15p, recruits two F-actin nucleation pathways to coordinate cytokinetic actin ring formation in Schizosaccharomyces pombe. The Journal of cell biology. 2003; 162:851–862. [PubMed: 12939254]

Chen JS, Broadus MR, McLean JR, Feoktistova A, Ren L, Gould KL. Comprehensive proteomics analysis reveals new substrates and regulators of the fission yeast clp1/cdc14 phosphatase. Molecular & cellular proteomics : MCP. 2013; 12:1074–1086. [PubMed: 23297348]

Clifford DM, Wolfe BA, Roberts-Galbraith RH, McDonald WH, Yates JR 3rd, Gould KL. The Clp1/Cdc14 phosphatase contributes to the robustness of cytokinesis by association with anillin-related Mid1. The Journal of cell biology. 2008; 181:79–88. [PubMed: 18378776]

Cortes JC, Carnero E, Ishiguro J, Sanchez Y, Duran A, Ribas JC. The novel fission yeast (1,3)beta-D-glucan synthase catalytic subunit Bgs4p is essential during both cytokinesis and polarized growth. Journal of cell science. 2005; 118:157–174. [PubMed: 15615781]

Cortes JC, Ishiguro J, Duran A, Ribas JC. Localization of the (1,3)beta-D-glucan synthase catalytic subunit homologue Bgs1p/Cps1p from fission yeast suggests that it is involved in septation, polarized growth, mating, spore wall formation and spore germination. Journal of cell science. 2002; 115:4081–4096. [PubMed: 12356913]

Cortes JC, Sato M, Munoz J, Moreno MB, Clemente-Ramos JA, Ramos M, Okada H, Osumi M, Duran A, Ribas JC. Fission yeast Ags1 confers the essential septum strength needed for safe gradual cell abscission. The Journal of cell biology. 2012; 198:637–656. [PubMed: 22891259]

Daga RR, Lahoz A, Munoz MJ, Moreno S, Jimenez J. Etd1p is a novel protein that links the SIN cascade with cytokinesis. The EMBO journal. 2005; 24:2436–2446. [PubMed: 15933715]

De Matteis MA, Luini A. Exiting the Golgi complex. Nature reviews Molecular cell biology. 2008; 9:273–284.

Fankhauser C, Reymond A, Cerutti L, Utzig S, Hofmann K, Simanis V. The S. pombe cdc15 gene is a key element in the reorganization of F-actin at mitosis. Cell. 1995; 82:435–444. [PubMed: 7634333]

Ge W, Balasubramanian MK. Pxl1p, a paxillin-related protein, stabilizes the actomyosin ring during cytokinesis in fission yeast. Molecular biology of the cell. 2008; 19:1680–1692. [PubMed: 18272786]

Hachet O, Simanis V. Mid1p/anillin and the septation initiation network orchestrate contractile ring assembly for cytokinesis. Genes & development. 2008; 22:3205–3216. [PubMed: 19056897]

Jaulin F, Xue X, Rodriguez-Boulan E, Kreitzer G. Polarization-dependent selective transport to the apical membrane by KIF5B in MDCK cells. Developmental cell. 2007; 13:511–522. [PubMed: 17925227]

Laporte D, Coffman VC, Lee IJ, Wu JQ. Assembly and architecture of precursor nodes during fission yeast cytokinesis. The Journal of cell biology. 2011; 192:1005–1021. [PubMed: 21422229]

Le Goff X, Utzig S, Simanis V. Controlling septation in fission yeast: finding the middle, and timing it right. Current genetics. 1999a; 35:571–584. [PubMed: 10467001]

Le Goff X, Woollard A, Simanis V. Analysis of the cps1 gene provides evidence for a septation checkpoint in Schizosaccharomyces pombe. Molecular & general genetics : MGG. 1999b; 262:163–172. [PubMed: 10503548]

Lee IJ, Wu JQ. Characterization of Mid1 domains for targeting and scaffolding in fission yeast cytokinesis. Journal of cell science. 2012; 125:2973–2985. [PubMed: 22427686]

Liu J, Tang X, Wang H, Oliferenko S, Balasubramanian MK. The localization of the integral membrane protein Cps1p to the cell division site is dependent on the actomyosin ring and the septation-inducing network in Schizosaccharomyces pombe. Molecular biology of the cell. 2002; 13:989–1000. [PubMed: 11907277]

Liu J, Wang H, McCollum D, Balasubramanian MK. Drc1p/Cps1p, a 1,3-beta-glucan synthase subunit, is essential for division septum assembly in Schizosaccharomyces pombe. Genetics. 1999; 153:1193–1203. [PubMed: 10545452]

Martin-Garcia R, Valdivieso MH. The fission yeast Chs2 protein interacts with the type-II myosin Myo3p and is required for the integrity of the actomyosin ring. Journal of cell science. 2006; 119:2768–2779. [PubMed: 16772338]

Martin SG, Berthelot-Grosjean M. Polar gradients of the DYRK-family kinase Pom1 couple cell length with the cell cycle. Nature. 2009; 459:852–856. [PubMed: 19474792]

Mishra M, Karagiannis J, Sevugan M, Singh P, Balasubramanian MK. The 14-3-3 protein rad24p modulates function of the cdc14p family phosphatase clp1p/flp1p in fission yeast. Current biology : CB. 2005; 15:1376–1383. [PubMed: 16085489]

Moseley JB, Mayeux A, Paoletti A, Nurse P. A spatial gradient coordinates cell size and mitotic entry in fission yeast. Nature. 2009; 459:857–860. [PubMed: 19474789]

Pardo M, Nurse P. Equatorial retention of the contractile actin ring by microtubules during cytokinesis. Science. 2003; 300:1569–1574. [PubMed: 12791993]

Park JS, Steinbach SK, Desautels M, Hemmingsen SM. Essential role for Schizosaccharomyces pombe pik1 in septation. PloS one. 2009; 4:e6179. [PubMed: 19587793]

Pinar M, Coll PM, Rincon SA, Perez P. Schizosaccharomyces pombe Pxl1 is a paxillin homologue that modulates Rho1 activity and participates in cytokinesis. Molecular biology of the cell. 2008; 19:1727–1738. [PubMed: 18256290]

Pollard LW, Onishi M, Pringle JR, Lord M. Fission yeast Cyk3p is a transglutaminase-like protein that participates in cytokinesis and cell morphogenesis. Molecular biology of the cell. 2012; 23:2433–2444. [PubMed: 22573890]

Pollard TD, Wu JQ. Understanding cytokinesis: lessons from fission yeast. Nature reviews Molecular cell biology. 2010; 11:149–155.

Qualmann B, Kelly RB. Syndapin isoforms participate in receptor-mediated endocytosis and actin organization. The Journal of cell biology. 2000; 148:1047–1062. [PubMed: 10704453]

Roberts-Galbraith RH, Chen JS, Wang J, Gould KL. The SH3 domains of two PCH family members cooperate in assembly of the Schizosaccharomyces pombe contractile ring. The Journal of cell biology. 2009; 184:113–127. [PubMed: 19139265]

Roberts-Galbraith RH, Ohi MD, Ballif BA, Chen JS, McLeod I, McDonald WH, Gygi SP, Yates JR 3rd, Gould KL. Dephosphorylation of F-BAR protein Cdc15 modulates its conformation and stimulates its scaffolding activity at the cell division site. Molecular cell. 2010; 39:86–99. [PubMed: 20603077]

Samejima I, Miller VJ, Rincon SA, Sawin KE. Fission yeast Mto1 regulates diversity of cytoplasmic microtubule organizing centers. Current biology : CB. 2010; 20:1959–1965. [PubMed: 20970338]

Sammons MR, James ML, Clayton JE, Sladewski TE, Sirotkin V, Lord M. A calmodulin-related light chain from fission yeast that functions with myosin-I and PI 4-kinase. Journal of cell science. 2011; 124:2466–2477. [PubMed: 21693583]

Sawin KE, Lourenco PC, Snaith HA. Microtubule nucleation at non-spindle pole body microtubule-organizing centers requires fission yeast centrosomin-related protein mod20p. Current biology : CB. 2004; 14:763–775. [PubMed: 15120067]

Takeda T, Kawate T, Chang F. Organization of a sterol-rich membrane domain by cdc15p during cytokinesis in fission yeast. Nature cell biology. 2004; 6:1142–1144.

Trautmann S, Wolfe BA, Jorgensen P, Tyers M, Gould KL, McCollum D. Fission yeast Clp1p phosphatase regulates G2/M transition and coordination of cytokinesis with cell cycle progression. Current biology : CB. 2001; 11:931–940. [PubMed: 11448769]

Tsujita K, Suetsugu S, Sasaki N, Furutani M, Oikawa T, Takenawa T. Coordination between the actin cytoskeleton and membrane deformation by a novel membrane tubulation domain of PCH proteins is involved in endocytosis. The Journal of cell biology. 2006; 172:269–279. [PubMed: 16418535]

Valente C, Turacchio G, Mariggio S, Pagliuso A, Gaibisso R, Di Tullio G, Santoro M, Formiggini F, Spano S, Piccini D, et al. A 14-3-3gamma dimer-based scaffold bridges CtBP1-S/BARS to PI(4)KIIIbeta to regulate post-Golgi carrier formation. Nature cell biology. 2012; 14:343–354.

Venkatram S, Tasto JJ, Feoktistova A, Jennings JL, Link AJ, Gould KL. Identification and characterization of two novel proteins affecting fission yeast gamma-tubulin complex function. Molecular biology of the cell. 2004; 15:2287–2301. [PubMed: 15004232]

Vjestica A, Tang XZ, Oliferenko S. The actomyosin ring recruits early secretory compartments to the division site in fission yeast. Molecular biology of the cell. 2008; 19:1125–1138. [PubMed: 18184749]

Wachtler V, Huang Y, Karagiannis J, Balasubramanian MK. Cell cycle-dependent roles for the FCH-domain protein Cdc15p in formation of the actomyosin ring in Schizosaccharomyces pombe. Molecular biology of the cell. 2006; 17:3254–3266. [PubMed: 16687577]

Walch-Solimena C, Novick P. The yeast phosphatidylinositol-4-OH kinase pik1 regulates secretion at the Golgi. Nature cell biology. 1999; 1:523–525.

Wu JQ, Kuhn JR, Kovar DR, Pollard TD. Spatial and temporal pathway for assembly and constriction of the contractile ring in fission yeast cytokinesis. Developmental cell. 2003; 5:723–734. [PubMed: 14602073]

Wu JQ, Pollard TD. Counting cytokinesis proteins globally and locally in fission yeast. Science. 2005; 310:310–314. [PubMed: 16224022]

Yamaguchi H, Hiratani T, Baba M, Osumi M. Effect of aculeacin A, a wall-active antibiotic, on synthesis of the yeast cell wall. Microbiology and immunology. 1985; 29:609–623. [PubMed: 2935715]

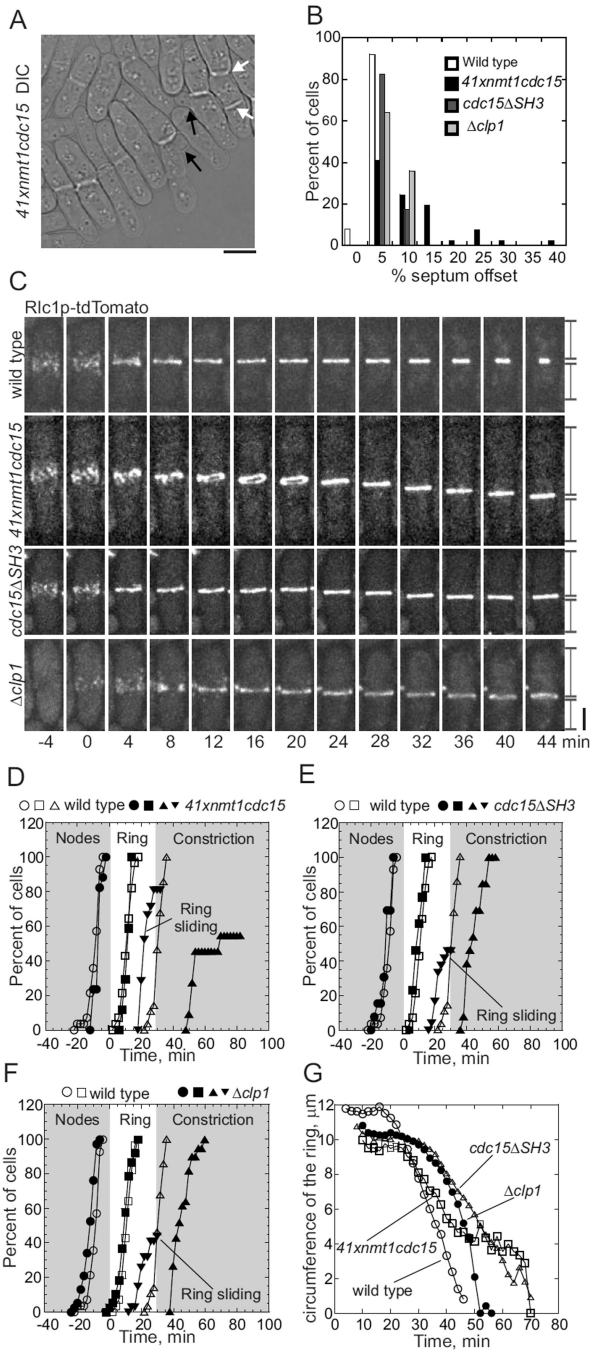

Figure 1. Comparison of cytokinesis in three mutant strains

Imaging in all figures was done at 25°C on 25% gelatin pads in EMM5S unless specified otherwise. Time zero in all figures is defined by the separation of the spindle pole bodies. (A) A DIC image of *41xnmt1cdc15* cells depleted of Cdc15p by incubation with 2.8 μM thiamine in EMM5S for 24 h at 25°C and with 2.8 μM thiamine in the gelatin pad. A white arrow highlights a cell with two septa and black arrows highlight branched cells. Scale bar 5 μm.

(B) Histogram of the positions of septa measured as the percent offset from the cell center: (white bars) wild type cells (n = 24); (black bars) cells depleted of Cdc15p (n = 41); (dark grey bars) *cdc15ΔSH3* cells with Cdc15p lacking the SH3 domain (n = 80); and (light grey bars) Δ*clp1* cells (n = 31).

(C) Time series of fluorescence micrographs (maximum intensity projections of 19 z-slices, 4 min intervals) of cells expressing Rlc1p-tdTomato. First panel, a wild type cell with a centrally located contractile ring that began to constrict at +24 min. Second panel, a cell depleted of Cdc15p with a contractile ring that moved toward the lower pole beginning at +16 min. Third panel, a *cdc15ΔSH3* cell with a contractile ring that moved toward the lower pole at +20 min. Fourth panel, a Δ*clp1* cell with a contractile ring that moved toward the lower pole beginning at time 20 min. Vertical lines at the end of time series mark the lengths of the daughter cells Scale bar 2 μm.

(D – F) Time courses of (O, ●) appearance of cortical nodes tracked with Rlc1p-tdTomato, (□, ■) completion of contractile rings, (Δ,▲) onset of ring constriction and (▼) ring sliding. (Open symbols) wild type cells (same data used in D-F) and (filled symbols) mutant cells.

(D) Wild type (O, □, n = 24 and Δ, n = 29) and cells depleted of Cdc15p (●, ■, n = 10, ▲, n = 9, ▼ n = 17).

(E) Wild type and *cdc15ΔSH3* cells (●, ■, ▼ n = 32; ▲, n = 24).

(F) Wild type and Δ*clp1* cells (●, ■,▲, ▼, n = 34).

(G) Time course of contractile ring constriction measured as the circumference of Rlc1ptdTomato fluorescence in (O, n = 12) wild type cells, (□, n = 9) cells depleted of Cdc15p, (Δ, n = 9) *cdc15ΔSH3* and (●, n = 21) Δ*clp1* cells.

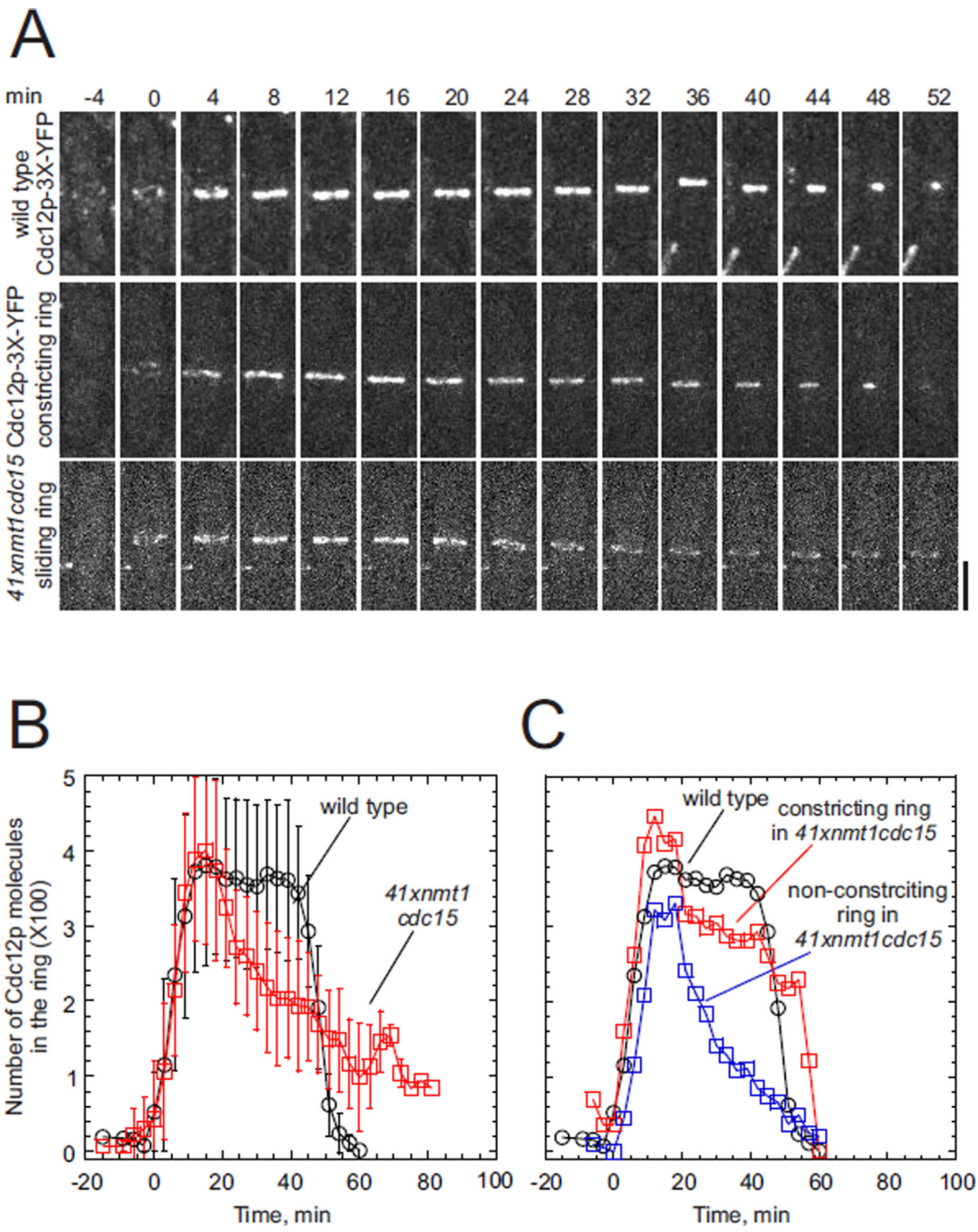

Figure 2. Recruitment of formin Cdc12p to nodes and contractile rings

(A) Time series of fluorescence micrographs (maximum intensity projections of 20 z-slices, 4 min intervals) of cells expressing Cdc12p-3YFP. Top panel, a wild type cell with a centrally located contractile ring that began to constrict at time 24 min. Middle panel, a cell depleted of Cdc15p with a contractile ring that constricted completely. Bottom panel, a cell depleted of Cdc15p with a contractile ring that moved toward the bottom pole beginning at time 18 min, failed to constrict and then disassembled. Scale bar 2 μm.

(B and C) Time courses of the accumulation and loss of Cdc12p-3YFP molecules (mean ± 1 SD) at the cleavage site at 25°C. (black O) wild type cells (n = 13).
(B) (red □) whole sample of *41xnmt1cdc15* (n = 10) cells depleted of Cdc15p.
(C) (blue □ with dashed line) one cell depleted of Cdc15p with a ring that disassembled after failing to constrict and (red □ with dashed line) one Cdc15p depleted cell with a constricting ring.

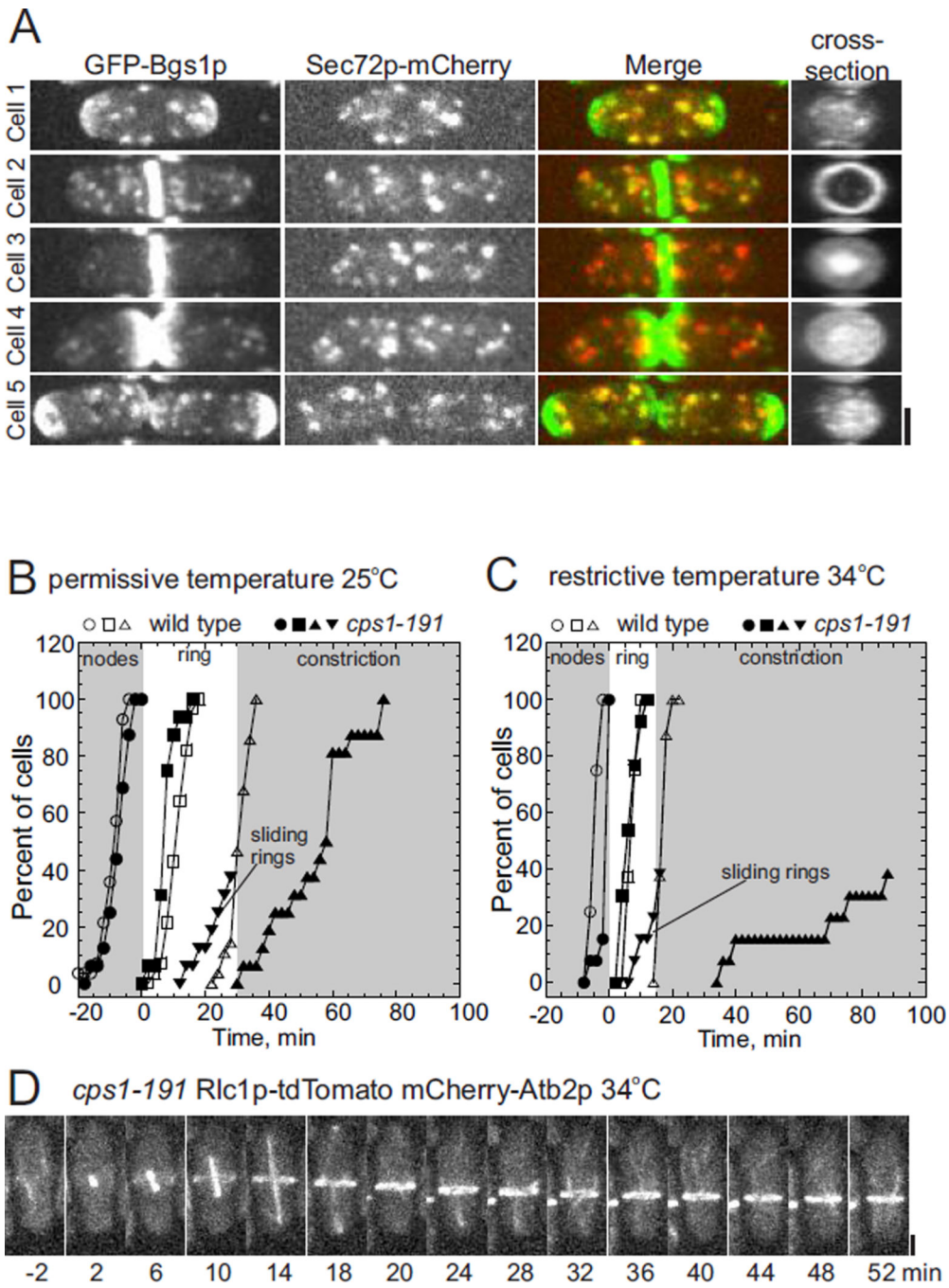

Figure 3. Bgs1p localization and its role in contractile ring anchoring

(A) Fluorescence micrographs (maximum intensity projections of 18 confocal z-slices) of five different wild type cells expressing (first column) GFP-Bgs1p, (second column) Sec72p-mCherry. The third column is a merge of the two fluorescence images. Fourth column is cross-section views of GFP-Bgs1p in the middle of the top cell and the cleavage furrows of the other cells. Cell 1, interphase; Cell 2, early cytokinesis; Cell 3, late cytokinesis; Cell 4, newly divided daughter cells; Cell 5, daughter cells growing at old ends.

(B and C) Time course of cytokinesis tracked with Rlc1p-tdTomato in (open symbols) wild type cells and (filled symbols) temperature sensitive Bgs1p mutant *cps1–191*. (O, ●) appearance of Rlc1p-tdTomato in nodes; (□, ■) completion of the contractile ring; (Δ, ▲) onset of contractile ring constriction; and (▼) onset of ring sliding.

(B) Time course of cytokinesis at 25°C (O, n = 14; ●, n = 16); (□, n = 14; ■ n = 16); (Δ, n = 9;▲, n = 16) and (▼ n=11).

(C) Time course of cytokinesis at 34°C: (O, n = 14; ●, n = 13); (□, n = 14; ■ n = 13); (Δ, n = 9;▲, n = 13) and (▼ n=13).

(D) Time series of fluorescence micrographs (maximum intensity projection of 18 confocal z-slices, 4 min intervals) at 34°C of a *cps1–191* cell expressing Rlc1p-tdTomato and mCherry-Atb2p (tubulin). Spindle microtubules appear at time 0 min. The contractile ring slid toward the lower pole at time 14 min. Scale bar 2 μm.

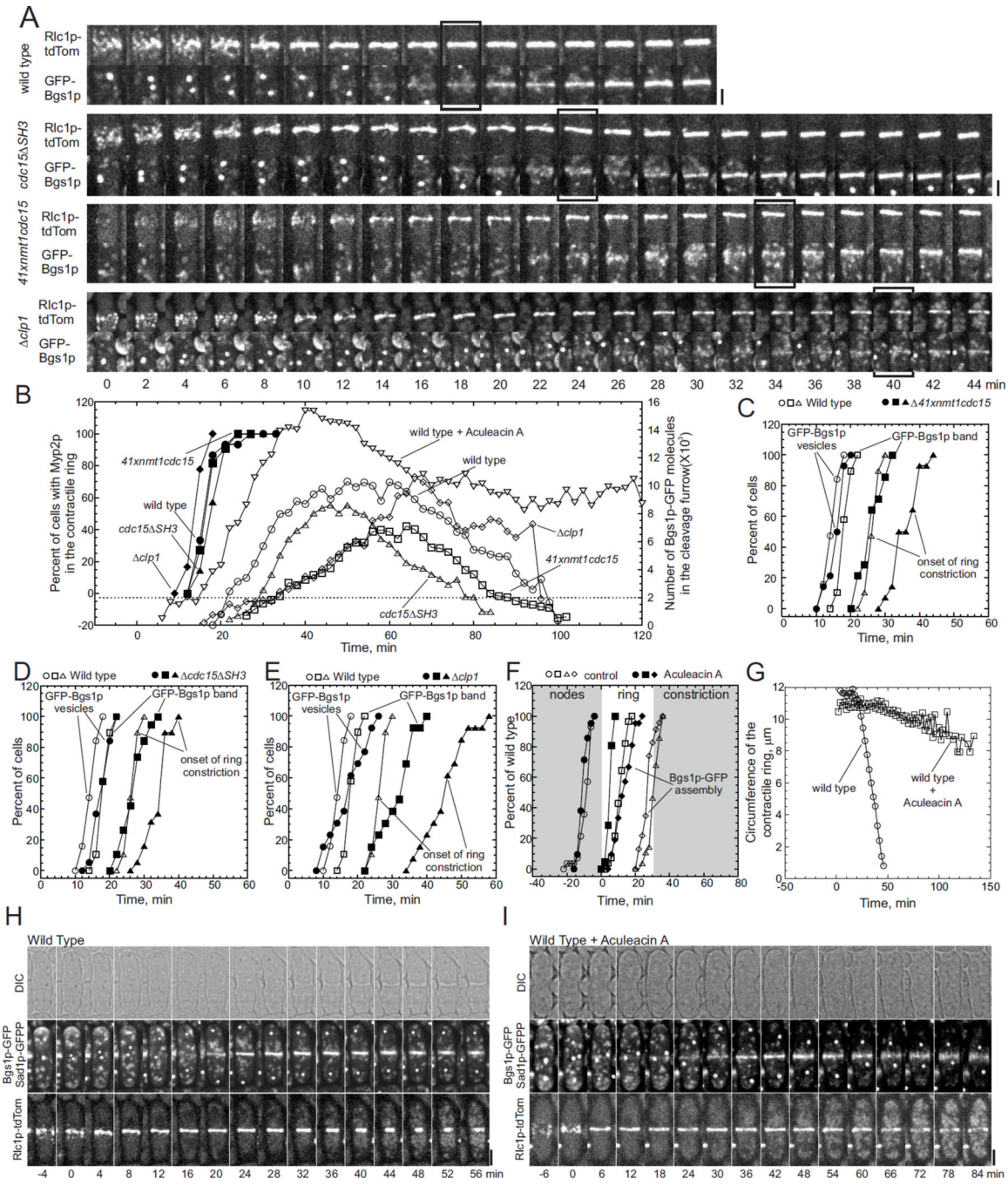

Figure 4. Bgs1p accumulates slowly around the equator of *cdc15* mutant cells

(A) Time series of fluorescence micrographs (maximum intensity projections of 18 confocal z-slices, 2 min intervals) of four strains expressing (upper panels) Rlc1p-tdTomato to mark contractile rings, and (lower panels) GFP-Bgs1p to mark primary septa and Sad1p-GFP to mark spindle pole bodies. Each image is a 40 × 40 pixel ROI of the cell center. First panel, wild type cells; second panel, *cdc15ΔSH3* cells; third panel, cells depleted of Cdc15p; and fourth panel, Δ*clp1* cells. Boxes mark when GFP-Bgs1p formed a ring.

(B) Time courses of appearance of Myp2p-YFP in contractile rings and numbers of GFP-Bgs1p molecules in cleavage furrows. (Left Y-axis, filled symbols) Appearance of Myp2p-YFP in contractile rings of (●, n = 17) wild type cells, (■, n = 11) Cdc15p depleted cells, (▲, n = 17) *cdc15*Δ*SH3* cells and (◆, n = 19) Δ*clp1* cells. (Right Y-axis, open symbols) Average numbers of GFP-Bgs1p molecules around the equators of (O, n = 15) wild type cells, (□, n = 12) cells depleted of Cdc15p, (Δ, n = 19) *cdc15*Δ*SH3* cells, (◊, n = 12) Δ*clp1* cells and (▽, n=12) wild type cells incubated with 320 μM Aculeacin A. GFP-Bgs1p fluorescence intensities were measured in 20-optical sections at 2 min intervals for 2 h, normalized and corrected for background.

(C – E) Time courses of (O, ●) appearance of Golgi vesicles containing GFP-Bgs1p at the cell center, (□, ■) appearance of GFP-Bgs1p rings and (Δ, ▲) onset of contractile ring constriction tracked with Rlc1p-tdTomato. (Open symbols) all three graphs use the same data for wild type cells (n = 19). (Filled symbols) mutant cells.

(C) Wild type and cells depleted of Cdc15p (n = 14). (D) Wild type and *cdc15*Δ*SH3* cells lacking the C-terminal SH3 domain (n = 19).

(E) Wild type and Δ*clp1* cells (n = 13).

(F–I) Effects of Aculeacin A on cytokinesis.

(F) Time course of cytokinesis in wild type cells expressing Rlc1p-tdTomato, GFP-Bgs1p and Sad1p-GFP preincubated for 15 min with (open symbols) 380 mM dimethyl sulfoxide (DMSO) or (filled symbols) with 320 μM Aculeacin A in DMSO prior to imaging with DMSO or Aculeacin A. Events: (O, n = 14; ●, n = 21) appearance of Rlc1p-tdTomato in nodes; (□, n = 14; ■, n=21) contractile ring formation; (◇, n = 15; ◆, n = 21) appearance of a band of GFP-Bgs1p around the equator; and (Δ, n = 14) onset of contractile ring constriction.

(G) Time course of contractile ring constriction measured as the circumference of Rlc1p-tdTomato fluorescence in wild type cells (O, n = 12) with 380 mM DMSO or (□, n = 21) 320 μM Aculeacin A in DMSO.

(H – I) Time series of (upper panel) DIC images and (middle and lower panels) maximum intensity projected fluorescent images of wild type cells expressing GFP-Bgs1p and Sad1p-GFP and Rlc1p-tdTomato showing the formation of (middle panel) a septum and (lower panel) a contractile ring from nodes.

(H) Wild type cells treated with 380 mM DMSO. Scale bar 2 μm.

(I) Wild type cells treated with 320 μM Aculeacin A in DMSO. Scale bar 2 μm.

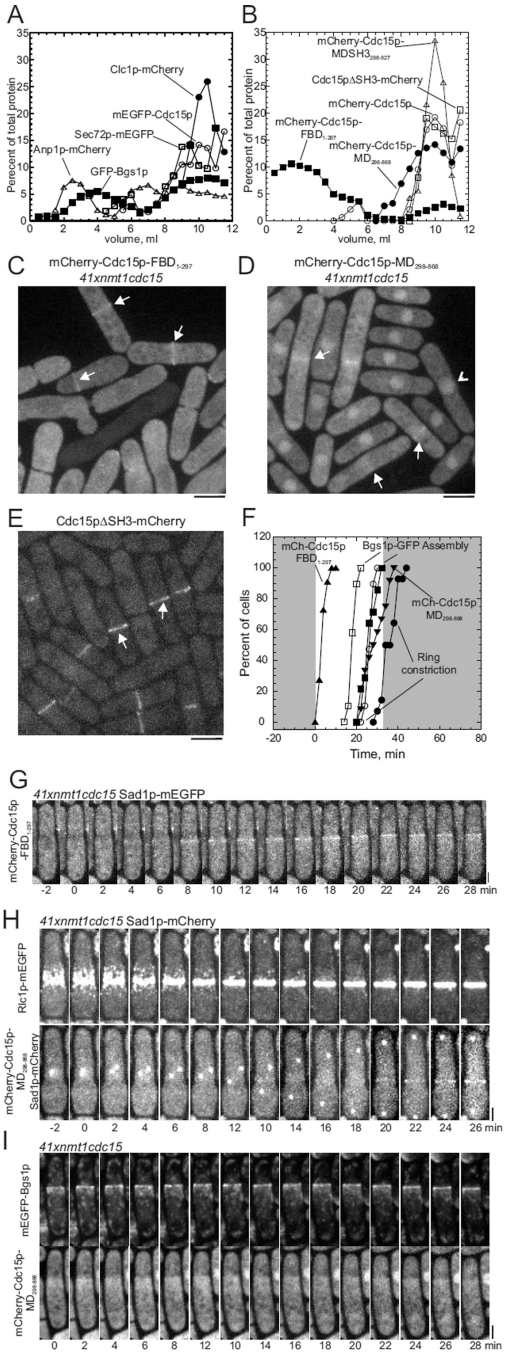

Figure 5. Cellular distribution and domain analysis of Cdc15p

(A) Sedimentation velocity ultracentrifugation of homogenates of wild type cells expressing either cis-Golgi marker Anp1p-mCherry, mEGFP-Cdc15p, GFP-Bgs1p, clathrin light chain Clc1p-mCherry or *trans*-Golgi marker Sec72p-mEGFP. Homogenate samples of 1 ml were centrifuged on 12 ml gradients of 18%–60% sucrose for 140 min at 38,000 rpm at 4°C. Fractions of 250 μl were (fraction 1 is the top of the gradient) analyzed by SDS-PAGE and quantitative immunoblotting: (■) GFP-Bgs1p; (□) Sec72p-mEGFP; (O) mEGFP-Cdc15p; (▲) Clc1p-mCherry and (Δ) Anp1p-mCherry.

(B–I) Domain analysis using truncation mutations of Cdc15p expressed in cells depleted of Cdc15p: mCherry-Cdc15pMDSH3$_{298–927}$ lacking the F-BAR domain; mCherry-Cdc15pFBD$_{1–297}$ consisting of only the F-BAR domain; and mCherry-Cdc15pMD$_{298–868}$ consisting of only the middle domain and Cdc15pΔSH3-mCherry consisting of the F-BAR domain and the middle domain expressed in wild type cells.

(B) Sedimentation velocity ultracentrifugation as in (A) except that fractions were 500 μl. Symbols: (O) mCherry-Cdc15p; (□) Cdc15pΔSH3-mCherry; (Δ) mCherry-Cdc15pMDSH3$_{298–927}$; (●) mCherry-Cdc15pMD$_{298–868}$; and (■) mCherry-Cdc15pFBD$_{1–297}$.

(C – E) Maximum intensity projections of images of 20 confocal z-slices (Δz = 0. 36) of mCherry fluorescence from truncation mutants of Cdc15p.

(C) Cells depleted of Cdc15p and expressing mCherry-Cdc15p-FBD$_{1–297}$. White arrows highlight fluorescent bands. Nodes are not visible over the high background fluorescence.

(D) Cells depleted of Cdc15p expressing mCherry-Cdc15p-MD$_{298–868}$. White arrows highlight broad zones of fluorescence in mitotic cells and arrowheads mark interphase nuclei.

(E) Cells expressing Cdc15pΔSH3-mCherry and mEGFP-Bgs1p (not shown). Arrows highlight fluorescence in contractile rings. (F) Time courses of (O, ●) onset of contractile ring constriction tracked with Rlc1p-tdTomato, and formation of rings of (□, ■) GFP-Bgs1p, (▲) mCherry-Cdc15p FBD$_{1–297}$ and (▼) mCherry-Cdc15p-MD$_{298–868}$. (Open symbols) wild type cells (n = 29) and (filled symbols) cells depleted of Cdc15p (●, ■ n = 10, ▲ n = 12 and ▼ n = 11).

(G–I) Time series of fluorescence micrographs (maximum intensity projections of 20 z-slices, 2 min intervals) of cells depleted of Cdc15p expressing fluorescent fusion proteins. The contrast was digitally enhanced to visualize the weak signals. Scale bars 2 μm.

(G) Sad1p-mEGFP and mCherry-Cdc15p FBD$_{1–297}$.

(H) (Upper row) Rlc1p-mEGFP and (lower row) Sad1p-mCherry and mCherry-Cdc15p-MD$_{298–868}$.

(I) (Upper row) mEGFP-Bgs1p and (lower row) mCherry-Cdc15p-MD$_{298–868}$.

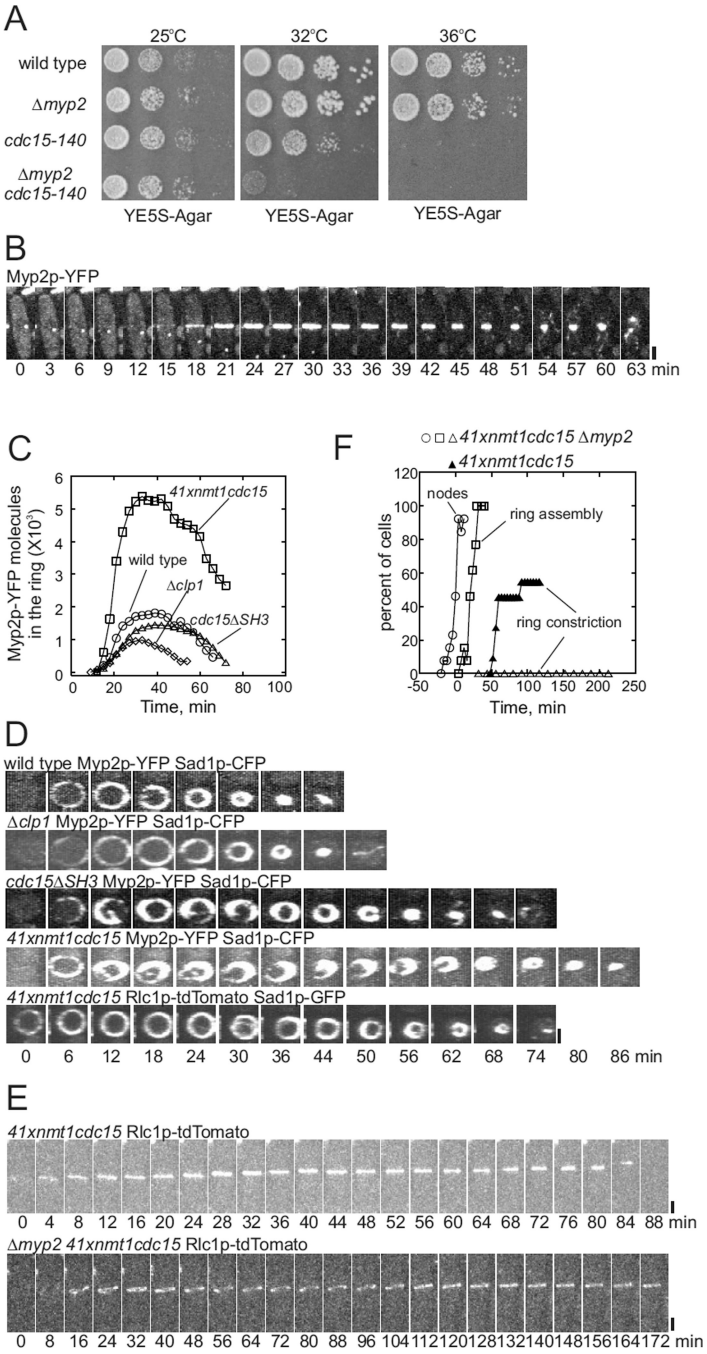

Figure 6. Sliding of contractile rings in cells depleted of Cdc15p depends on Myp2p

(A) Growth of serial dilutions of wild type and mutant strains Δ*myp2*, *cdc15–140* and Δ*myp2 cdc15–140* for 3 d at 25°C, 32°C or 36°C.

(B) Time series of fluorescence micrographs (maximum intensity projection of 19 confocal z-slices at 3 min intervals) of a cell expressing Myp2p-YFP and Sad1p-CFP (not shown).

(C) Time course of the accumulation and disappearance of Myp2p-YFP molecules (mean numbers) in contractile rings of (O, n = 17) wild type cells, (□, n = 11) cells depleted of

Cdc15p, (Δ, n = 17) *cdc15*Δ*SH3* cells and (◇, n = 19) Δ*clp1* cells also expressing Sad1p-CFP.

(D) Time series of fluorescence micrographs showing elongated structures containing myosins separating from contractile rings in *cdc15* mutants. Images of 20 Z sections were collected every 3 min and reconstructed into sections across the mid plane of the each cell. First row: wild type cells expressing Myp2p-YFP and Sad1p-CFP. Second row: Δ*clp1* cells expressing Myp2p-YFP and Sad1p-CFP. Third row: *cdc15*Δ*SH3* cells expressing Myp2p-YFP and Sad1p-CFP. Fourth row: cells depleted of Cdc15p expressing Myp2p-YFP and Sad1p-CFP. Fifth row: cells depleted of Cdc15p expressing Rlc1p-TdTomato and Sad1p-GFP.

(E) Time series of fluorescence micrographs (maximum intensity projection of 19 confocal z-slices, 8 min intervals) of cells expressing Rlc1p-tdTomato and Sad1p-GFP and released from the S-phase block by hydroxyurea 2 h prior to imaging. (Upper panel) cell depleted of Cdc15p, (lower panel) a cell depleted of Cdc15p and lacking Myp2p. Scale bars 2 μm.

(F) Time course of cytokinesis tracked with Rlc1p-tdTomato in (filled symbols) cells depleted of Cdc15p and (open symbols) cells depleted of Cdc15p and lacking Myp2p: (○, n = 14) appearance of Rlc1p-tdTomato in nodes; (□, n = 14) contractile ring completed; and (▲, n = 14; Δ, n = 9) onset of contractile ring constriction. Data from every 12th min was represented.

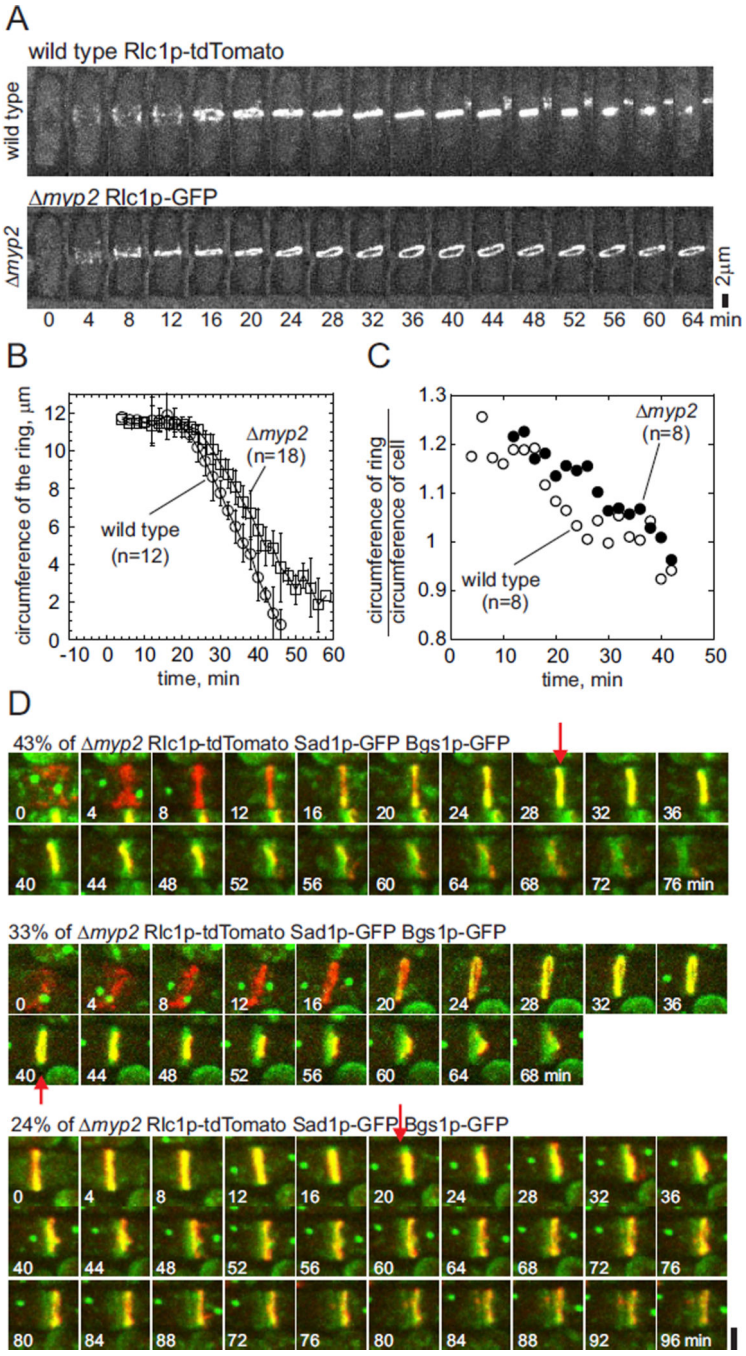

Figure 7. Cytokinesis defects in Δ*myp2* deletion mutants

(A) Time series of fluorescence micrographs of (upper panel) wild type cells and (lower panel) Δ*myp2* mutant cells expressing Rlc1p-tdTomato and Sad1p-GFP. These are maximum intensity projections of 19 confocal z-slices at 4 min time intervals. Scale bar 2 μm.

(B) Time course of contractile ring constriction measured as the average circumference of Rlc1p-tdTomato contractile rings ±1 SD in (O, n = 12) wild type cells and (□, n = 18) Δ*myp2* cells.

(C) Time course of the ratio between circumference of Rlc1p-tdTomato contractile rings and the circumference of the cleavage furrow (GFP-Bgs1p) in (O, n = 8) wild type cells and (●, n = 8) Δ*myp2* mutant cells expressing Rlc1p-tdTomato, GFP-Bgs1p and Sad1p-GFP and imaged in 19 z-slices with 0.36 μm spacing every 2 min for 2 h at 25°C.
(D) Time series of merged fluorescence micrographs (maximum intensity projection of 19 confocal z-slices, 4 min intervals) of Δ*myp2* mutant cells expressing Rlc1p-tdTomato to mark contractile rings, Sad1p-GFP to mark spindle pole bodies and GFP-Bgs1p to mark primary septa (n = 51). Images are the middles (45 × 45 pixels) of cells with the long axis horizontal. The upper panel is representative of 43% of cells with coordinated rings and septa. The middle panel is representative of 33% of cells with the contractile ring and associated Bgs1p displaced to one side of the furrow where the septum grew and closed ahead of the contractile ring. The lower panel is representative of 24% of cells where the septum appeared to close and separate the daughter cells, while the ring regressed. The first image in each time series is at arbitrary time 0 min. The red arrows indicate the first appearance of asymmetry in the GFP-Bgs1p distribution. Scale bar 2 μm.